Novel natural non-nucleoside inhibitors of HIV-1 reverse transcriptase identified by shape- and structure-based virtual screening techniques

*Giosuè Costa,[#‡] Roberta Rocca,[#‡] Angela Corona,[§] Nicole Grandi,[§] Federica Moraca,[*ξ#] Isabella Romeo,[#] Carmine Talarico,[#] Maria Giovanna Gagliardi,[#] Francesca Alessandra Ambrosio,[#] Francesco Ortuso,[#] Stefano Alcaro,[#] Simona Distinto,[‖] Elias Maccioni,[‖] Enzo Tramontano[§] and Anna Artese[#]*

[#]Dipartimento di Scienze della Salute, Università degli Studi "Magna Græcia" di Catanzaro, Campus "S. Venuta", Viale Europa, Germaneto, 88100, Catanzaro, Italy.

[§]Dipartimento di Scienze della Vita e dell'Ambiente, Università di Cagliari, Cittadella Universitaria di Monserrato, SS554, 09042 Monserrato, Cagliari, Italy.

[‖]Dipartimento di Scienze della Vita e dell'Ambiente, Università degli Studi di Cagliari, Via Ospedale 72, 09124, Cagliari, Italy.

[ξ] Department of Chemical Sciences, University of Napoli Federico II, Via Cinthia 4, I-80126 Napoli, Italy.

‡These authors contributed equally.

ABSTRACT: In this work we report a parallel application of both docking- and shape-based virtual screening (VS) methods, followed by Molecular Dynamics simulations (MDs), for discovering new compounds able to inhibit the human immunodeficiency virus type 1 (HIV-1) reverse transcriptase (RT) RNA-dependent DNA polymerase activity. Specifically, we screened more than 143000 natural compounds commercially available in the ZINC database against the best five RT crystallographic models, taking into account the five approved NNRTIs as query compounds. As a result, 20 *hit* molecules were selected and tested on biochemical assays for the inhibition of the RNA dependent DNA polymerase RT function and, among them, an indoline pyrrolidine (*hit* **1**), an indonyl piperazine (*hit* **2**) and an indolyl indolinone (*hit* **3**) derivatives were identified as novel non-nucleoside RT inhibitors in the low micromolar range.

KEYWORDS: Reverse transcriptase; NNRTIs; *in silico* virtual screening; natural products.

INTRODUCTION

Human immunodeficiency virus (HIV) is a retrovirus that can lead to acquired immunodeficiency syndrome (AIDS). HIV primarily infects vital CD4+ cells in the human immune system, such as helper T cells, macrophages and dendritic cells. When CD4+ T cell numbers decline below a critical level, cell-mediated immunity is lost, and the body becomes progressively more susceptible to opportunistic infections.[1] Several host and virological factors determine the extremely variable rates of disease progression that are observed among HIV-infected individuals. Once entered, HIV is able to replicate in a six steps life cycle: (1) Binding and fusion (2) Reverse transcription (3) Integration (4) Transcription (5) Assembly (6) Budding.

Reverse Transcriptase (RT) is the most characterized target of HIV: it plays a major role in viral replication, since it converts the viral single-stranded RNA into proviral double stranded DNA.[2] Both nucleoside (NRTIs) and non-nucleoside RT (NNRTIs) inhibitors represent an important group of drugs in the treatment of HIV. Indeed, for newly diagnosed individuals with HIV, two NRTIs, such as tenofovir disoproxil fumarate (TDF) and emtricitabine (FTC), and either a NNRTI, such as efavirenz (EFV), a boosted protease inhibitor or an integrase strand transfer inhibitor are recommended according to the current guidelines for first-line therapy.[3] In HIV treatment, other combinations of NRTIs and NNRTIs are also effective and considered first line,[4] thus highlighting the importance of the so called "Highly Active Antiretroviral Therapy" (HAART).[5] With respect to NRTIs, NNRTIs have the advantage of higher potency, lower toxicity, higher selectivity and specificity.[6] Despite the remarkable successes of current therapies, antiviral drug resistance severely limits the efficacy of long-term treatment regimens due to continuous viral replication and prolonged exposure to the drugs, thus impairing the effectiveness of the combined drugs.[3] The successive selection of additional mutations can lead to multidrug resistance that dramatically affects the outcome of HAART,[7] enlightening the need of a constant effort to identify novel inhibitors.[8-10] Additionally, new antiretroviral agents are under development to attempt to improve the pharmaceutical properties of the drugs, with the aim to achieve better dosing profiles, minimize side effect profiles and increase the efficacy.[11]

Even natural extracts are investigated as a promising source of antiviral agents,[12-16] and several natural molecules have been extensively studied as new antiretroviral agents, such as the epigallocatechin gallate, an allosteric RT inhibitor acting with different mechanisms from those of the approved NNRTIs,[17] as well as some guttiferone A analogues, extracted from *Clusiaceae* and developed as effective NNRTIs to treat drug resistant HIV-1.[18]

In the demanding process of drug discovery, an accurate rational design of new agents is still of considerable importance and, in particular, molecules derived from natural plants could provide precious structural alternatives to optimize the drugs combination treatment regimen in the HIV disease.

In the last decades, virtual screening (VS) approaches proved to be important tools in medicinal chemistry to speed up the drug discovery process.[19,20] Several success stories have been reported,[21,22,23] even if VS methods are not immune to pitfalls and weakness.[20,24,25] In particular, remarkable difficulties have been encountered in structure-based *de novo* design of NNRTI scaffolds. Some publications reported that this allosteric binding site often undergoes more marked structural rearrangements upon binding than those of active site and this can create some problems when structure based methods are applied.[26,27] However, by considering more crystal structures (i.e with an ensemble docking protocol), this limitation can be reduced, so that several studies where ligand-based and structure based methods have been applied were able to successfully retrieve new NNRTIs.[28,29,30] Moreover, in order to minimize these limitations, docking and similarity search results are usually combined to further increase compound recall of individual methods.[31,32] According to Tan and co-workers, when both the similarity searching and docking results are integrated, a parallel selection of candidate compounds from individual rankings is generally superior to rank fusion. Thus, with the aim to find new NNRTI lead structures for HIV-1 RT, we applied a parallel docking and a shape-based virtual screening on 143758 natural compounds commercially available in the ZINC database against the best five RT crystallographic models, taking into account the five approved NNRTIs as query compounds. We finally identified 20 promising best *hits*, further tested in terms of their RT inhibitory activity. Among them, an indoline pyrrolidine (*hit* **1**), an indonyl piperazine (*hit* **2**) and an indolyl

indolinone (*hit* **3**), investigated in detail by means of molecular dynamics simulations, were able to inhibit the enzyme RNA-dependent DNA polymerase activity in the micromolar range, thus opening the way to a new approach for RT drug development.

RESULTS AND DISCUSSION

In order to consider the NNRTI binding pocket flexibility, we applied an ensemble docking approach by investigating the molecular recognition of the 1702 compounds (active and decoys sets) against 40 RT models complexed to the five approved drugs (for details see Supplementary Material Table S1) and, based on the enrichment factor (EF) analysis, we selected the RT models associated to the highest AUC values and to the greatest number of active compounds (for details see Supplementary Material Table S2). Therefore, we identified 1FKP,[33] 1IKW,[34] 1KLM,[35] 3M8P[36] and 4KFB[37] as best models, respectively in complex with nevirapine (NVP), efavirenz (EFV), delavirdine (DLV), etravirine (ETV) and rilpivirine (RPV).

The five best RT models obtained after the validation procedure were used for virtually screening the library of 143758 natural compounds. In particular, by applying in parallel docking- and shape-based approaches, we identified a different number of ligands. Specifically, after the structure-based analysis, for each RT model, we selected the 100 top scored compounds according to their G-score value with respect to the best pose, thus globally obtaining 500 compounds. From the ligand-based approach, we selected 8694 molecules with a shape similarity score higher than 0.6 with respect to the bioactive conformation of the five approved NNRTIs. Finally, by merging these results, we identified the 20 shared compounds reported in Table 1.

N°	ZINC Code	2D structure	GScore *(kcal/mol)*	Shape sim - Query
1	ZINC62001555	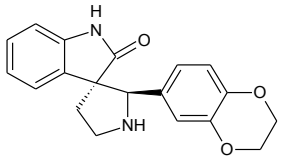	-10.23	0.61 - NVP
2	ZINC40312945	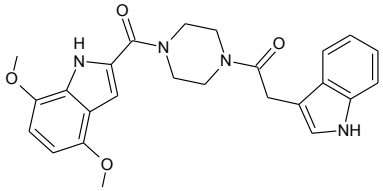	-13.05	0.64 - DLV
3	ZINC20759448	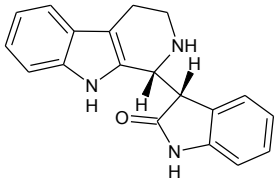	-10.21	0.62 - NVP
4	ZINC00303740	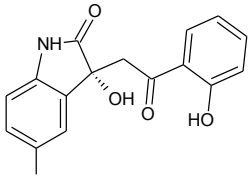	-10.28	0.61 - NVP
5	ZINC12296720	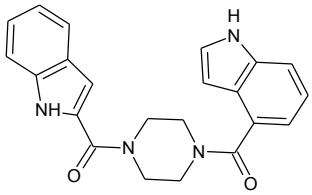	-13.49	0.71 - DLV
6	ZINC02131155	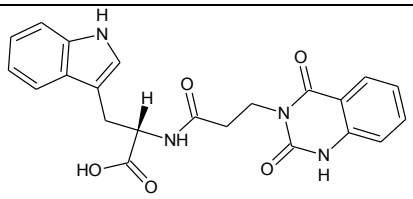	-12.94	0.63 - DLV

7	ZINC00565262	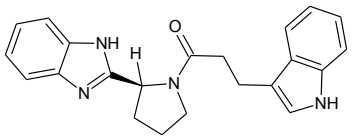	-11.21	0.60 - ETV
8	ZINC08764773	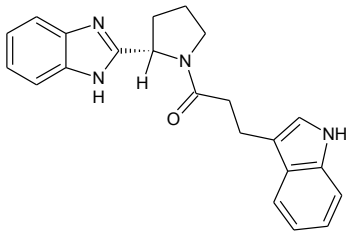	-10.95	0.60 - ETV
9	ZINC20111634	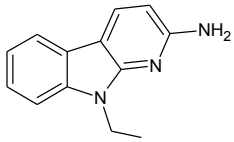	-10.19	0.72 - NVP
10	ZINC03985118	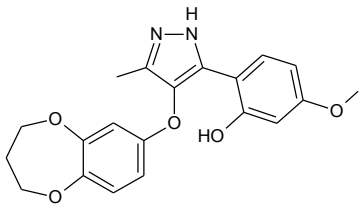	-11.77	0.66 - ETV
11	ZINC05013091	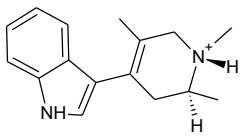	-11.79	0.62 - ETV 0.62 - RPV
12	ZINC05184432	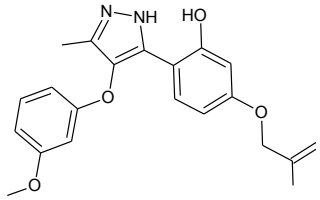	-11.26	0.63 - ETV

13	ZINC08565325	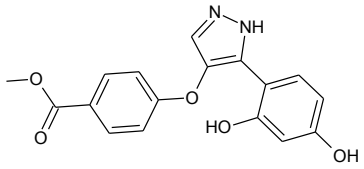	-11.07	0.60 - ETV 0.63 - RPV
14	ZINC08973599	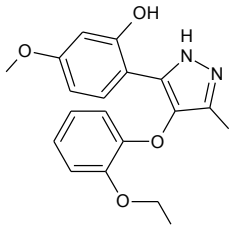	-11.08	0.61 - ETV
15	ZINC08995112	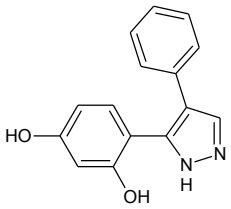	-10.43	0.61 - ETV 0.63 - NVP
16	ZINC13549561	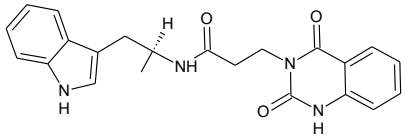	-12.72	0.62 - DLV
17	ZINC18006781	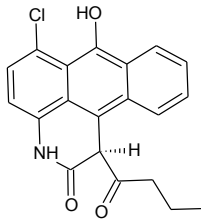	-11.79	0.63 - ETV
18	ZINC18145162	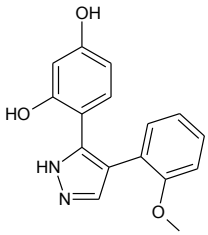	-10.23	0.62 - ETV 0.66 - NVP 0.61 - RPV

19	ZINC18270702	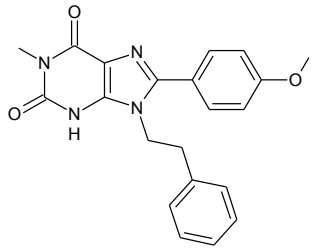	-11.24	0.66 - ETV 0.67 - RPV
20	ZINC20762321	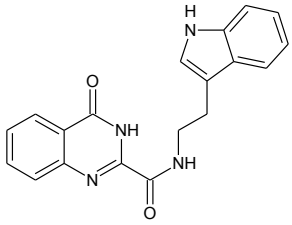	-11.40	0.62 - ETV 0.67 - DLV 0.60 - RPV

Table 1. 2D representation, ZINC code, Glide score (G-Score) value and Shape similarity Score (Shape sim - Query), calculated with respect to the related query, of the shared best 20 *hits* identified by combining the ligand-based and the structure-based virtual screening approaches. G-scores values are expressed in kcal/mol.

We further analyzed the *drug-like* properties of the best *hits* and we observed that all of them satisfied the Lipinski's rule of five (RO5) (for full details, see Supplementary Material Figure S1). The conformational properties of the 20 promising screened compounds were very diversified, as evidenced by the number of their rotatable bonds, and most of them presented a Polar Surface Area (PSA) < 100, allowing to predict a good oral absorption.[38]

These best *hits* were purchased from different vendors and tested for their effect on the HIV-1 RT inhibition activity (Table 2), using the NNRTI EFV as reference compound.

N°	**ZINC Code**	**HIV-1 RDDP IC_{50}** *(μM)*[a]
1	ZINC62001555	40.3 ± 2.5
2	ZINC40312945	59.4 ± 7.1
3	ZINC20759448	9.75 ± 0.02
4	ZINC00303740	>100 (88%)[b]

5	ZINC12296720	>100 (62%)
6	ZINC02131155	>100 (100%)
7	ZINC00565262	>100 (85%)
8	ZINC08764773	>100 (79%)
9	ZINC20111634	>100 (77%)
10	ZINC03985118	>100 (72%)
11	ZINC05013091	89.5 ± 0.2
12	ZINC05184432	86.4 ± 13.9
13	ZINC08565325	100 ± 1
14	ZINC08973599	71.0 ± 1.44
15	ZINC08995112	>100 (65%)
16	ZINC13549561	>100 (73%)
17	ZINC18006781	78.2± 9.9
18	ZINC18145162	>100 (61%)
19	ZINC18270702	>100 (96%)
20	ZINC20762321	>100 (63%)
Efavirenz	EFV	0.024 ± 0.005

[a] compound concentration able to inhibit the 50% of the RNA dependent DNA polymerase activity of HIV-1 Reverse Transcriptase enzyme.
[b] percentage of enzymatic activity in presence of 100uM inhibitor.

Table 2. Biological effects of selected compounds on HIV-1 RT RNA dependent DNA polymerase activity.

Out of the 20 tested compounds, seven of them inhibited the HIV-1 RDDP function with different potencies. In particular, six of them showed IC_{50} values ranging from 40 μM (compound **1**) to 89 μM (compound **11**), and one (compound **3**), being significantly more potent (IC_{50} 9.75 ± 0.02 μM). **3** is a derivative of the 1,2,3,4-tetrahydro-β-carboline, an alkaloid extracted from the fruit of *Plectocomiopsis geminiflorus* (*Palmae*) and could be considered a molecular simplification of the marine alkaloids manzamines, associated to antimicrobial,

pesticidal, anti-inflammatory and antiviral properties.[39-44] The molecule has a peculiar structure, that conjugates a big tetrahydro-pyrido-indolyl group, suggested as potential constituent of HIV-1 inhibitors by *in-silico* studies,[45] with an indolinone ring. The indolinone moiety was also present in the scaffold of **1**, the second most effective *hit* that showed an IC_{50} value of 40 μM, included in a spiro-indole-pyrrolidine ring system, that is typical of many pharmacologically relevant alkaloids, such as vincristine, vinblastine[46] and spirotryprostatins.[47] This compound is the derivative of natural compounds and it was been synthesized on the base of Horsfiline, an alkaloid obtained from the leaves of *Phalaris coerulescens*. The third most potent inhibitor was **2**, a natural semi-synthetic compound characterized by a dimethoxy-indole-2-carbonyl-piperazinyl-indolyl scaffold that showed an IC_{50} of 59 μM. In order to better understand the interactions with the HIV-1 RT and have some insights that could lead to future structure optimization, we analyzed the binding modes of the lowest energy pose of the three most active compounds (Figure 1). We observed that **3** and **1** were docked into the RT active site of 1FKP PDB model, while **2** was well accommodated in the 1KLM binding pocket. Specifically, in this last X-ray model, a water molecule was placed into the NNI pocket and was involved in an hydrogen bond bridging the backbone nitrogen of p66 K101 with the side chain of E138 of the p51 subunit. As already observed for the co-crystallized ligand in 1KLM model, **2** was not able to interact with this water molecule, though showing a similar orientation into the binding pocket. As shown in Figure 1A, the complex was further stabilized by an additional hydrogen bond between the ligand carbonyl group with the amide group of K103 and by two stacking interactions with W229. Interestingly, one of **2** derivatives was reported in literature as integrase inhibitor,[32] paving the way for further molecular and biological studies focused on this scaffold to optimize its potential dual activity.

Compound **1** in complex with HIV-1 RT was stabilized by two stacking interactions established with Y318 and W229 and one hydrogen bond between the ligand amide group and the backbone carbonyl moiety of K101. Finally, the protonated amino group of **1** interacted with the side chain of E138 through a salt bridge interaction, thus enhancing the stability of the complex (Figure 1B).

The best experimental *hit*, the tetrahydro-pyrido-indolyl-indolinone **3** exhibited a binding mode similar to that of **1**, with the exception of the salt bridge, substituted by a hydrogen bond between the ligand amido group and the side chain carboxylic group of E138 (Figure 1C). In particular, we observed some favorable stacking interactions among the aromatic ring of the β-carboline and the RT residues Y188 and W229 and one hydrogen bond between the ligand carbonyl group and the backbone nitrogen of K101.

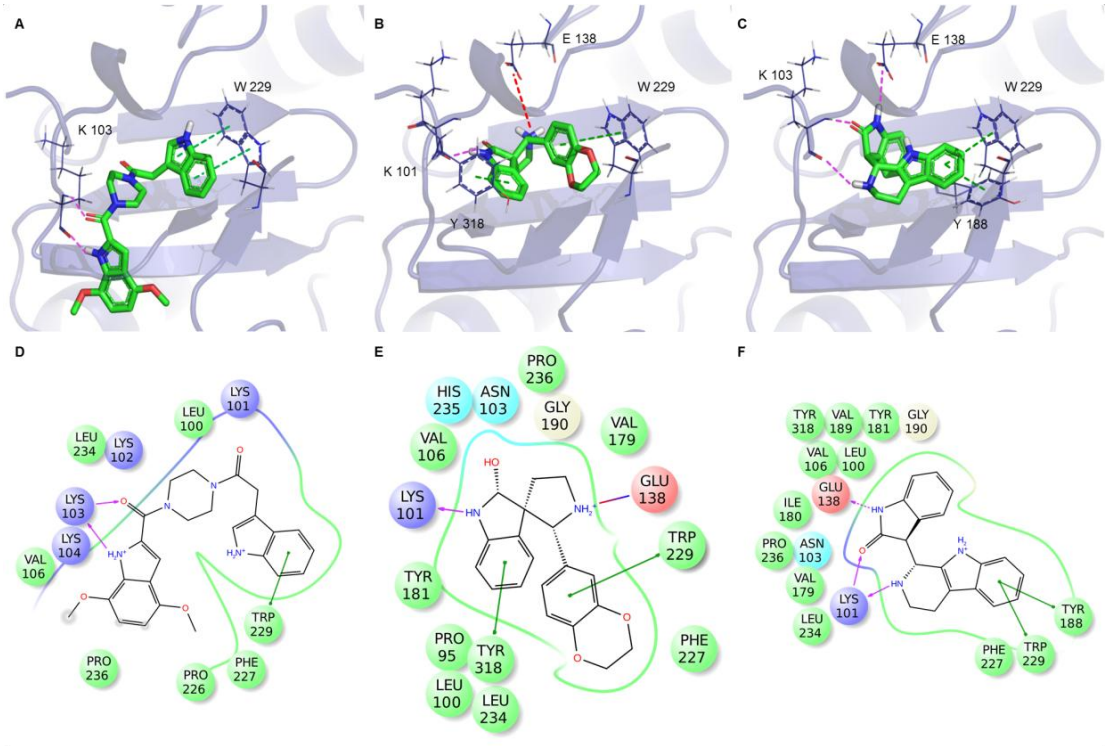

Figure 1. 3D and 2D representations of the lowest energy pose of (**A-D**) **2** (PDB code: 1KLM), (**B-E**) **1** (PDB code: 1FKP) and (**C-F**) **3** (PDB code: 1FKP) docked into the RT binding pocket. In 3D representation, ligand is depicted as green carbon sticks, the RT is shown as slate transparent cartoon and the enzyme residues involved in crucial contacts with the compounds are reported as slate carbon lines. Both in 3D and 2D representations, hydrogen bonds, stacking interactions and salt bridges are shown, respectively, as dashed violet, green and red lines.

As reported in Figure S1, according to their *drug-like* properties, the three active compounds could represent potential candidate drugs, since they perfectly conformed to the RO5. In particular, among them, the most active **3** is ranked among the less flexible compounds, with only one possible rotatable bond, and it is also associated to good theoretical pharmacokinetic properties, satisfying both Polar Surface Area and AlogP descriptors.

Finally, in order to refine the docking results, we submitted the complex of the three most active molecules to Molecular Dynamics simulations (MDs) and, with the aim to investigate their binding mode into the HIV-RT pocket during the time, we monitored the single contributions of hydrophobic, water bridges, π- π and hydrogen bonding interactions with respect to those of the co-crystallized ligands.

As reported in Figure S2, we noticed that **2**, the best found *hit* in complex with 1KLM model, engaged an increased number of hydrophobic contacts with L100, V106, Y181, Y188, F227, W229 and Y318, if compared to those of the co-crystallized inhibitor DLV. Although the number of hydrogen bonds of the best *hit* in complex with the enzyme was lower than that of DLV, the favorable binding energy profile of this molecule with respect to the known inhibitor was compensated by a greater number of π-π interactions with Y181, Y188 and W229 (Table 3 and Figure S3 of the Supplementary Material).

As concerns **3**, if compared to the co-crystallized inhibitor NVP (model 1FKP), we observed a higher frequency of hydrogen bonds, hydrophobic and water bridges interactions due to the presence of the indolinone moiety. In particular, the screened compound was involved in a major

number of hydrogen bonds with K101 and E138 and hydrophobic contacts with Y188, F227, L234 and Y318 (for full details, see Supplementary Material Figure S4). Such a structural observation was further confirmed by its thermodynamic profile that revealed a strong binding affinity of the compound into the binding pocket of HIV-1 RT (Table 3 and Figure S5 of the Supplementary Material).

Concerning **1**, as reported in Figure S4, we found an increased number of hydrogen bond between the compound and E138, P236, Y318 residues, and of π-π interactions with Y183, Y188, F227 and W229. In addition, with respect to that of NVP, we observed a higher number of contacts between the RT hydrophobic core formed by the side chains of P95, V106, V108, Y188, F227, L234 residues and the compound.

Average ΔG_{bind}	*1KLM*		*1FKP*		
	DLV	*Hit* **2**	NVP	*Hit* **3**	*Hit* **1**
	-77.16	-79.30	-51.74	-65.03	-143.76

Table 3. Average ΔG_{bind} values of the known NNRTIs and the three most active screened molecules monitored during the MDs. The energy values are expressed in kcal/mol.

EXPERIMENTAL SECTION

Active compounds. The active compounds used in this study were obtained from the ChEMBL database.[48] We firstly indicated the HIV-1 reverse transcriptase as target and then selected, from various literature sources, 50 molecules with IC_{50} values lower than 20 nM. Moreover, in the active set we included also the five approved NNRTIs, that are delavirdine, efavirenz, nevirapine, etravirine and rilpivirine, thus globally obtaining 55 molecules. In Table S3, the ChEMBL code, the SMILES chemical formula[49] and the IC_{50} values of the active

compounds are reported. The decoys set was generated by using the DUD-E database,[50] starting from the active compounds and applying a ratio of 30:1, thus obtaining 1647 molecules.

All the molecules used as test sets were submitted to 10000 iterations of full energy minimization adopting the Polake-Ribiere Conjugated Gradient (PRCG) algorithm and the "all atoms" notation of the OPLS_2005 force field,[51] as implemented in the MacroModel suite ver. 11.0.[52] Solvent effects were considered by adopting the implicit solvation model GB/SA water.[53] The optimization process was performed up to the derivative convergence criterion of 0.05 kcal $Å^{-1} \cdot mol^{-1}$.

Database of natural compounds. The high throughput *in silico* approach was conducted by virtually screening 143758 natural compounds publicly available in the ZINC[54] repository associated with twelve vendor companies (AfroDb Natural Products,[55] Analyticon Discovery NP,[56] Herbal Ingredients In-Vivo Metabolism,[57] IBScreen NP,[58] Indofine Natural Products,[59] NPACT Database,[60] Nubbe Natural Products,[61] Princeton NP,[62] Specs Natural Products,[63] TCM Database @ Taiwan,[64] UEFS Natural Products[65]).

All the molecules included in such database were prepared considering the ionization state at physiological 7.0 ± 1.0 pH and all the tautomeric and protomeric forms were energy minimized using the OPLS_2005 force field, as implemented in the LigPrep platform ver. 2.9[66] of Maestro. Qikprop software, implemented in the Schrodinger Suite, was adopted to estimate pharmaceutically relevant properties, such as compound solubility, permeability and many others, that are potentially important in the drug development process.[67] Finally, they were filtered basing on their *drug-like* properties as it has been addressed by the Lipinski's rule of five[68] and the duplicated structures were removed. A total amount of 165838 compounds successfully passing this filter were subjected to the further molecular recognition process.

Protein preparation. Based on the availability in the Protein Data Bank (PDB)[69] and on the related resolution, we downloaded 40 crystallographic structures of the HIV-1 RT complexed to the five approved drugs (for details see Supplementary Material Table S1).

After removing the ligands, all the receptors were refined and energy optimized using the Protein Preparation Wizard tool.[70] Hydrogen atoms were added and the geometry of all the hetero groups was corrected.

Glide redocking and docking protocol. Based on the enrichment factor and the AUC analyses, among the 40 RT structures, we selected the five models, one for each known non-nucleoside inhibitor, able to better discriminate among active and decoys molecules (1702 compounds) and we used them as receptors to test the accuracy and reliability of the docking procedure (for details, see Supplementary Material Figures S6-S10). We performed Glide ver. 6.9[71] redocking calculations starting from the five best RT co-crystallized models (PDB ID 1FKP, 1IKW, 1KLM, 3M8P and 4KFB, respectively) in order to geometrically reproduce the experimental data. Glide grids were generated by Receptor Grid Generation; the grid box volume of all receptors was 64000 $Å^3$ and it was centered onto the co-crystallized ligand. We used Glide Standard Precision (SP) protocol with default parameters, generating ten poses for each ligand. For all complexes, the program was able to well reproduce the experimental geometries with RMSD values always below 0.5 Å (for full details, see Supplementary Material Table S4).

Consequently, we started from the best RT models as receptors for the further docking-based virtual screening of the database of natural compounds, adopting the same parameters of the validation procedure.

Shape Screening. By using Phase method,[72] based on the principle of rapid initial alignments using atom triplets followed by refinement and volume overlap scoring, we applied a screening

shape-based (SBVS) approach of the database of natural compounds by using the bioactive conformation of the five approved NNRTIs as reference molecules. In order to score the screening molecules, we adopted the option that combines shape and atom properties, and, for atom typing in the shape search, we used MacroModel types (Shape_MMod). We prepared all structures by using LigPrep ver. 2.9 and we further performed the shape similarity search. For each molecule in the database, up to 100 conformers were generated by means of the ConfGen[73] tool, implemented in the MacroModel suite, and the shape of each conformer was then compared with that of the query structures. A normalized shape similarity value was computed for each conformer relative to that of the query structure, with 0 indicating dissimilarity and 1 the same shapes.[74] Finally, we filtered out all conformers with similarity below 0.6.

Molecular Dynamics. The co-crystallized ligands and the most active molecules in complex with RT enzyme were submitted to 50 ns of Molecular Dynamics simulations by using Desmond ver. 4.4.[75] The complexes were solvated in an orthorhombic box with a buffer of 10 Å TIP4P water and 9 Cl^- ions were added to neutralize the system net charge. Prior to the MD runs, we relaxed the system with Martyna-Tobias_Klein isobaric-isothermal ensemble (MTK_NPT). This preliminary stage included two minimization simulations of 2000 steps: in the first run the complex was restrained with a force constant of 50 kcal $Å^{-1} \cdot mol^{-1}$, while in the second one all the system was released without any restraint. Afterwards, a first simulation with the NVT ensemble was carried out at 10K, meanwhile the three successive simulations were performed using the NPT ensemble, a temperature of 300K, a pressure of 1 bar with the Berendsen thermostat-barostat. The production phase of NPT MD was run for 50 ns, with a recording interval to 50 ps both for energy and trajectory and 1000 snapshot saved structures. The

Simulation Interaction Diagram and the Simulation Event Analysis were used to investigate the trajectories in terms of contacts and energy of interaction of the ligand within the enzyme.

Biochemical assays. Recombinant heterodimeric RT group M subtype B was expressed and purified as reported by Corona *et al*.[76] Briefly *E. coli* strain M15 containing the p6HRT-prot vector was grown to an optical density at 600 nm of 0.7 and induced with 1.7 mM isopropyl β-D-1-thiogalactopyranoside (IPTG) for 4 h. Protein purification was carried out with a BioLogic LP system (Biorad), using a combination of IMAC and ion exchange chromatography. Cell pellets were resuspended in lysis buffer (50 mM sodium phosphate buffer pH 7.8, containing 0.5 mg/mL lysozyme), incubated on ice for 20 min, and after adding NaCl to a final concentration of 0.3 M, were sonicated and centrifuged at 30,000×g for 1 h. A combined two-step purification was performed: the supernatant was loaded onto a Ni^{2+}-NTA-Sepharose column pre-equilibrated with loading buffer (50 mM sodium phosphate buffer pH 7.8, containing 0.3M NaCl, 10% glycerol, and 10 mM imidazole) and washed thoroughly with wash buffer (50 mM sodium phosphate buffer pH 6.0, containing 0.3 M NaCl, 10% glycerol, and 80 mM imidazole). RT was eluted with an imidazole gradient in wash buffer (0 – 0.5 M). Fractions were collected, protein purity was checked by SDS-PAGE and found to be higher than 90%. The 1:1 ration between the p66/p51 subunits was also verified. Enzyme-containing fractions were pooled and diluted 1:1 with 50 mM sodium phosphate buffer pH 7.0, containing 10% glycerol; and then loaded into a Hi-trap heparin HP GE (Healthcare Lifescience) pre-equilibrated with 10 column volumes of loading buffer (50 mM sodium phosphate buffer pH 7.0, containing 10% glycerol and 150 mM NaCl). The column was then washed with loading buffer and the RT was eluted with Elute Buffer 2 (50 mM Sodium Phosphate pH 7.0, 10% glycerol, 1 M NaCl). Fractions were collected, protein was dialyzed and stored in buffer containing 50 mM Tris HCl pH 7.0, 25 mM NaCl,

1mM EDTA, and 50% glycerol. Catalytic activities and protein concentrations were determined. Enzyme-containing fractions were pooled and aliquots were stored at -80 °C.

RNA-dependent DNA polymerase (RDDP) activity was measured as reported by Palomba *et al.*[77] in 25 µL volume containing 60 mM Tris HCl buffer pH 8.1, 8 mM $MgCl_2$, 60 mM KCl, 13 mM DTT, 2.5 µM poly(A)-oligo(dT), 100 µM dTTP, increasing concentrations of inhibitor, whose dilution were made in water, and different amounts of enzymes according to a linear range of dose-response curve. Reaction mixture was incubated for 30 min at 37 °C and the stopped by addition of 2 µl of 200 mM EDTA. Reaction products were detected by addition of 170 µl of revealing solution containing Picogreen in 10 mM Tris HCl pH 7.5, 1 mM EDTA, and measured with a multilabel counter plate reader Victor 3, equipped with filters 502/523 nm (excitation/emission wavelength).

ASSOCIATED CONTENT

Supplementary Material

Supplementary Material related to this article can be found at…

Author Contributions

The manuscript was written through contributions of all authors. All authors have given approval to the final version of the manuscript. Giosuè Costa and Roberta Rocca contributed equally.

AUTHOR INFORMATION

Corresponding Author:

*E-mail: fmoraca@unicz.it

ACKNOWLEDGMENTS

This research was supported by the Italian Ministry of Education (Funding for Investments of Base Research), code FIRB-IDEAS RBID082ATK.

ABBREVIATIONS

Human immunodeficiency virus (HIV), acquired immunodeficiency syndrome (AIDS), reverse transcriptase (RT), nucleoside (nucleotide) reverse transcriptase inhibitors (NRTIs), non-nucleoside (nucleotide) reverse transcriptase inhibitors (NNRTIs), C-C chemokine receptor type five (CCR5), tenofovir disoproxil fumarate (TDF), emtricitabine (FTC), efavirenz (EFV), Highly Active Antiretroviral Therapy (HAART), virtual screening (VS), nevirapine (NVP), delavirdine (DLV), etravirine (ETV) and rilpivirine (RPV), Lipinski's rule of five (RO5), Polar Surface Area (PSA), Molecular Dynamics simulations (MDs), Polake-Ribiere Conjugated Gradient (PRCG), Protein Data Bank (PDB), Standard Precision (SP), screening shape-based (SBVS), Martyna-Tobias_Klein isobaric-isothermal ensemble (MTK_NPT), isopropyl β-D-1-thiogalactopyranoside (IPTG), RNA-dependent DNA polymerase (RDDP).

REFERENCES

(1) Buchbinder, S. P.; Katz, M. H.; Hessol, N. A.; O'Malley, P. M.; Holmberg, S. D. Long-term HIV-1 infection without immunologic progression. *AIDS* **1994**, *8*, 1123-1128.

(2) Sarafianos, S. G.; Hughes, S. H.; Arnold, E. Designing anti-AIDS drugs targeting the major mechanism of HIV-1 RT resistance to nucleoside analog drugs. *Int J Biochem Cell Biol.* **2004**, *36*, 1706-1715.

(3) Cory, T. J.; Midde, N. M.; Rao, P.; Kumar, S. Investigational reverse transcriptase inhibitors for the treatment of HIV. *Expert Opin Investig Drugs* **2015**, *24*, 1219-1228.

(4) Greig, S. L.; Deeks, E. D. Elvitegravir/cobicistat/emtricitabine/tenofovir alafenamide: a review in HIV-1 infection. *Drugs* **2016**, *76*, 957-968.

(5) Brechtl, J. R.; Breitbart, W.; Galietta, M.; Krivo, S.; Rosenfeld, B. The use of highly active antiretroviral therapy (HAART) in patients with advanced HIV infection: impact on medical, palliative care, and quality of life outcomes. *J Pain Symptom Manage.* **2001**, *21*, 41-51.

(6) Bell, F. W.; Cantrell, A. S.; Hoegberg, M.; Jaskunas, S. R.; Johansson, N. G.; Jordan, C. L.; Kinnick, M. D.; Lind, P.; Morin, J. M. Phenethylthiazolethiourea (PETT) compounds, a new class of HIV-1 reverse transcriptase inhibitors. Synthesis and basic structure-activity relationship studies of PETT analogs. *J Med Chem.* **1995**, *38*, 4929-4936.

(7) Schneider, A.; Corona, A.; Sporing, I.; Jordan, M.; Buchholz, B.; Maccioni, E.; Di Santo, R.; Bodem, J.; Tramontano, E.; Wohrl, B. M. Biochemical characterization of a multi-drug resistant HIV-1 subtype AG reverse transcriptase: antagonism of AZT discrimination and excision pathways and sensitivity to RNase H inhibitors. *Nucleic acids research* **2016**, *44*, 2310-2322.

(8) Kang, D.; Fang, Z.; Li, Z.; Huang, B.; Zhang, H.; Lu, X.; Xu, H.; Zhou, Z.; Ding, X.; Daelemans, D.; De Clercq, E.; Pannecouque, C.; Zhan, P.; Liu, X. Design, Synthesis, and Evaluation of Thiophene[3,2-d]pyrimidine Derivatives as HIV-1 Non-nucleoside Reverse Transcriptase Inhibitors with Significantly Improved Drug Resistance Profiles. *J Med Chem.* **2016**, *59*, 7991-8007.

(9) Kang, D.; Fang, Z.; Huang, B.; Lu, X.; Zhang, H.; Xu, H.; Huo, Z.; Zhou, Z.; Yu, Z.; Meng, Q.; Wu, G.; Ding, X.; Tian, Y.; Daelemans, D.; De Clercq, E.; Pannecouque, C.; Zhan, P.; Liu, X. Structure-Based Optimization of Thiophene[3,2-d]pyrimidine Derivatives as Potent HIV-1

Non-nucleoside Reverse Transcriptase Inhibitors with Improved Potency against Resistance-Associated Variants. *J Med Chem.* **2017**, *60*, 4424-4443.

(10) Kang, D.; Ding, X.; Wu, G.; Huo, Z.; Zhou, Z.; Zhao, T.; Feng, D.; Wang, Z.; Tian, Y.; Daelemans, D.; De Clercq, E.; Pannecouque, C.; Zhan, P.; Liu, X. Discovery of Thiophene[3,2-d]pyrimidine Derivatives as Potent HIV-1 NNRTIs Targeting the Tolerant Region I of NNIBP. *ACS Med Chem Lett.* **2017**, *8*, 1188-1193.

(11) Gravatt, L. A. H.; Leibrand, C. R.; Patel, S.; McRae, M. New Drugs in the Pipeline for the Treatment of HIV: a Review. *Curr Infect Dis Rep.* **2017**, *19*, 42.

(12) Sonar, V. P.; Corona, A.; Distinto, S.; Maccioni, E.; Meleddu, R.; Fois, B.; Floris, C.; Malpure, N. V.; Alcaro, S.; Tramontano, E.; Cottiglia, F. Natural product-inspired esters and amides of ferulic and caffeic acid as dual inhibitors of HIV-1 reverse transcriptase. *Eur J Med Chem*. **2017**, *130*, 248-260.

(13) Esposito, F.; Mandrone, M.; Del Vecchio, C.; Carli, I.; Distinto, S.; Corona, A.; Lianza, M.; Piano, D.; Tacchini, M.; Maccioni, E.; Cottiglia, F.; Saccon, E.; Poli, F.; Parolin, C.; Tramontano, E. Multi-target activity of Hemidesmus indicus decoction against innovative HIV-1 drug targets and characterization of Lupeol mode of action. *Pathog Dis.* **2017**, *75*(6).

(14) Xu, L.; Grandi, N.; Del Vecchio, C.; Mandas, D.; Corona, A.; Piano, D.; Esposito, F.; Parolin, C.; Tramontano, E. From the traditional Chinese medicine plant Schisandra chinensis new scaffolds effective on HIV-1 reverse transcriptase resistant to non-nucleoside inhibitors. *J Microbiol.* **2015**, *53*, 288-293.

(15) Bicchi, C.; Rubiolo, P.; Ballero, M.; Sanna, C.; Matteodo, M.; Esposito, F.; Zinzula, L.; Tramontano, E. HIV-1 inhibiting activity of the essential oil of Ridolfia segetum and Oenanthe crocata. *Planta Medica* **2009**, *75*, 1-5.

(16) Kharlamova, T.; Esposito, F.; Zinzula, L.; Floris, G.; Cheng, Y. C.; Dutschman, G. E.; Tramontano, E. Inhibition of HIV-1 Ribonuclease H activity by novel frangula-emodine derivatives. *Medicinal Chemistry* **2009**, *5*, 398-410.

(17) Li, S.; Hattori, T.; Kodama, E. N. Epigallocatechin gallate inhibits the HIV reverse transcription step. *Antivir Chem Chemother.* **2011**, *21*, 239-243.

(18) Acuña, U. M.; Jancovski, N.; Kennelly, E. J. Polyisoprenylated benzophenones from Clusiaceae: potential drugs and lead compounds. *Curr Top Med Chem.* **2009**, *9*, 1560-1580.

(19) Kirchmair, J.; Distinto, S.; Schuster, D.; Spitzer, G.; Langer, T.; Wolber, G. Enhancing drug discovery through in silico screening: strategies to increase true positives retrieval rates. *Curr. Med. Chem.* **2008**, *15*, 2040-2053.

(20) Ripphausen, P.; Nisius, B.; Peltason, L.; Bajorath, J.r. Quo Vadis, virtual screening? A comprehensive survey of prospective applications. *J Med Chem.* **2010**, *53*, 8461-8467.

(21) Kubinyi, H. Success stories of computer-aided design, in: E. Sean (Ed.), Computer Applications in Pharmaceutical Research and Development, **2006**, pp. 377-424.

(22) Kirchmair, J.; Distinto, S.; Liedl, K. R.; Rollinger, J. M.; Markt, P.; Schuster, D.; Spitzer, G. M.; Wolber, G. Development of anti-viral agents using molecular modeling and virtual screening techniques. *Infect. Disord. Drug Targets* **2011**, *11*, 64-93.

(23) Distinto, S.; Esposito, F.; Kirchmair, J.; Cardia, M. C.; Gaspari, M.; Maccioni, E.; Alcaro, S.; Markt, P.; Wolber, G.; Zinzula, L.; Tramontano, E. Identification of HIV-1 reverse transcriptase dual inhibitors by a combined shape-, 2D-fingerprint- and pharmacophore-based virtual screening approach. *Eur J Med Chem.* **2012**, *50*, 216-229.

(24) Schneider, G. Virtual screening: an endless staircase? *Nat Rev Drug Discov.* **2010**, *9*, 273-276.

(25) Tiikkainen, P.; Markt, P.; Wolber, G.; Kirchmair, J.; Distinto, S.; Poso, A.; Kallioniemi, O. Critical comparison of virtual screening methods against the MUV data set. *J Chem Inf Model.* **2009**, *49*, 2168-2178.

(26) Paris, K. A.; Haq, O.; Felts, A. K.; Das, K.; Arnold, E.; Levy, R. M. Conformational Landscape of the Human Immunodeficiency Virus Type 1 Reverse Transcriptase Non-Nucleoside Inhibitor Binding Pocket: Lessons for Inhibitor Design from a Cluster Analysis of Many Crystal Structures. *J Med Chem.* **2009**, *52*, 6413-6420.

(27) Stanton, R. A.; Nettles, J. H.; Schinazi, R. F. Ligand similarity guided receptor selection enhances docking accuracy and recall for non-nucleoside HIV reverse transcriptase inhibitors. *J Mol Model.* **2015**, *21*, 282.

(28) Hosseini, Y.; Mollica, A.; Mirzaie, S. Structure-based virtual screening efforts against HIV-1 reverse transcriptase to introduce the new potent non-nucleoside reverse transcriptase inhibitor. *Journal of Molecular Structure* **2016**, *1125*, 592-600.

(29) Li, X.; Zhang, L.; Tian, Y.; Song, Y.; Zhan, P.; Liu, X. Novel HIV-1 non-nucleoside reverse transcriptase inhibitors: a patent review (2011 - 2014). *Expert Opin Ther Pat.* **2014**, *24*, 1199-1227.

(30) Ivetac, A.; Swift, S. E.; Boyer, P. L.; Diaz, A.; Naughton, J.; Young, J. A. T.; Hughes, S. H.; McCammon, J. A. Discovery of Novel Inhibitors of HIV-1 Reverse Transcriptase Through Virtual Screening of Experimental and Theoretical Ensembles. *Chem Biol Drug Des.* **2014**, *83*, 521-531.

(31) Tan, L.; Geppert, H.; Sisay, M.T.; Gutschow, M.; Bajorath, J. Integrating structure and ligand-based virtual screening: comparison of individual, parallel, and fused molecular docking and similarity search calculations on multiple targets. *ChemMedChem*. **2008**, *3*, 1566-1571.

(32) Alcaro, S.; Musetti, C.; Distinto, S.; Casatti, M.; Zagotto, G.; Artese, A.; Parrotta, L.; Moraca, F.; Costa, G.; Ortuso, F.; Maccioni, E.; Sissi, C. Identification and characterization of new DNA G-quadruplex binders selected by a combination of ligand and structure-based virtual screening approaches. *J Med Chem.* **2013**, *56*, 843-855.

(33) Ren, J.; Milton, J.; Weaver, K.L.; Short, S.A.; Stuart, D.I.; Stammers, D.K. Structural basis for the resilience of efavirenz (DMP-266) to drug resistance mutations in HIV-1 reverse transcriptase. *Structure Fold. Des.* **2000**, *8*, 1089-1094.

(34) Lindberg, J.; Sigurdsson, S.; Lowgren, S.; Andersson, H.O.; Sahlberg, C.; Noreen, R.; Fridborg, K.; Zhang, H.; Unge, T. Structural basis for the inhibitory efficacy of efavirenz (DMP-266), MSC194 and PNU142721 towards the HIV-1 RT K103N mutant. *Eur J Biochem.* **2002**, *269*, 1670-1677.

(35) Esnouf, R.M.; Ren, J.; Hopkins, A.L.; Ross, C.K.; Jones, E.Y.; Stammers, D.K.; Stuart, D.I. Unique features in the structure of the complex between HIV-1 reverse transcriptase and the bis(heteroaryl)piperazine (BHAP) U-90152 explain resistance mutations for this nonnucleoside inhibitor. *Proc Natl Acad Sci USA.* **1997**, *94*, 3984-3989.

(36) Kertesz, D.J.; Brotherton-Pleiss, C.; Yang, M.; Wang, Z.; Lin, X.; Qiu, Z.; Hirschfeld, D.R.; Gleason, S.; Mirzadegan, T.; Dunten, P.W.; Harris, S.F.; Villasenor, A.G.; Hang, J.Q.; Heilek, G.M.; Klumpp, K. Discovery of piperidin-4-yl-aminopyrimidines as HIV-1 reverse transcriptase inhibitors. N-benzyl derivatives with broad potency against resistant mutant viruses. *Bioorg Med Chem Lett.* **2010**, *20*, 4215-4218.

(37) Bauman, J.D.; Patel, D.; Dharia, C.; Fromer, M.W.; Ahmed, S.; Frenkel, Y.; Vijayan, R.S.; Eck, J.T.; Ho, W.C.; Das, K.; Shatkin, A.J.; Arnold, E. Detecting allosteric sites of HIV-1 reverse transcriptase by X-ray crystallographic fragment screening. *J Med Chem.* **2013**, *56*, 2738-2746.

(38) Oprea, T.I. Virtual Screening in Lead Discovery: A Viewpoint. *Molecules* **2002**, *7*, 51-62.

(39) Tintori, C.; Demeulemeester, J.; Franchi, L.; Massa, S.; Debyser, Z.; Christ, F.; Botta, M. Discovery of small molecule HIV-1 integrase dimerization inhibitors. *Bioorg Med Chem Lett.* **2012**, *22*, 3109-3114.

(40) Nakamura, H.; Deng, S.; Kobayashi, J. I.; Ohizumi, Y.; Tomotake, Y.; Matsuzaki, T.; Hirata, Y. Keramamine-A and-B, novel antimicrobial alkaloids from the Okinawan marine sponge Pellina sp. *Tetrahedron Letters* **1987**, *28*, 621-624.

(41) Peng, J.; Shen, X.; El Sayed, K.A.; Dunbar, D.C.; Perry, T.L.; Wilkins, S.P.; Hamann, M.T.; Bobzin, S.; Huesing, J.; Camp, R.; Prinsen, M.; Krupa, D.; Wideman, M.A. Marine natural products as prototype agrochemical agents. *J Agric Food Chem.* **2003**, *51*, 2246-2252.

(42) Edrada, R.A.; Proksch, P.; Wray, V.; Witte, L.; Müller, W.E.G.; Van Soest, R.W. Four new bioactive manzamine-type alkaloids from the Philippine marine sponge Xestospongia ashmorica. *J Nat Prod.* **1996**, *59*, 1056-1060.

(43) El Sayed, K.A.; Dunbar, D.C.; Perry, T.L.; Wilkins, S.P.; Hamann, M.T.; Greenplate, J.T.; Wideman, M.A. Marine natural products as prototype insecticidal agents. *J Agric Food Chem.* **1997**, *45*, 2735-2739.

(44) Peng, J.; Hu, J.F.; Kazi, A.B.; Li, Z.; Avery, M.; Peraud, O.; Hill, R.T.; Franzblau, S.G.; Zhang, F.; Schinazi, R.F.; Wirtz, S.S.; Tharnish, P.; Kelly, M.; Wahyuono, S.; Hamann, M.T. Manadomanzamines A and B: a novel alkaloid ring system with potent activity against mycobacteria and HIV-1. *J Am Chem Soc.* **2003**, *125*, 13382-13386.

(45) Penta, A.; Chander, S.; Ganguly, S.; Murugesan, S. De novo design and in-silico studies of novel 1-phenyl-2, 3, 4, 9-tetrahydro-1H-pyrido [3, 4-b] indole-3-carboxylic acid derivatives as HIV-1 reverse transcriptase inhibitors. *Medicinal Chemistry Research* **2014**, *23*, 3662-3670.

(46) Himes, R. H.; Kersey, R. N.; Heller-Bettinger, I.; Samson, F. E. Action of the vinca alkaloids vincristine, vinblastine, and desacetyl vinblastine amide on microtubules in vitro. *Cancer Research* **1976**, *36*, 3798-3802.

(47) Cui, C. B.; Kakeya, H.; Osada, H. Novel mammalian cell cycle inhibitors, spirotryprostatins A and B, produced by Aspergillus fumigatus, which inhibit mammalian cell cycle at G2/M phase. *Tetrahedron* **1996**, *52,* 12651-12666.

(48) ChEMBL. https://www.ebi.ac.uk/chembl

(49) Weininger, D. SMILES, a chemical language and information system. 1. Introduction to methodology and encoding rules. *J Chem Inf Model.* **1988**, *28*, 31-36.

(50) Mysinger, M. M.; Carchia, M.; Irwin, J. J.; Shoichet, B. K. Directory of useful decoys, enhanced (DUD-E): better ligands and decoys for better benchmarking. *J Med Chem.* **2012**, *55*, 6582-6594.

(51) Jorgensen, W.L.; Maxwell, D.S.; Tirado-Rives, J. Development and testing of the OPLS all-atom force field on conformational energetics and properties of organic liquids. *J Am Chem Soc.* **1996**, *118*, 11225-11236.

(52) Schrödinger Release 2015-4: MacroModel, Schrödinger, LLC, New York, NY, **2015**.

(53) Still, W.C.; Tempczyk, A.; Hawley, R.C.; Hendrickson, T. Semianalytical treatment of solvation for molecular mechanics and dynamics. *J Am Chem Soc.* **1990**, *112*, 6127-6129.

(54) Irwin, J.J.; Shoichet, B.K. ZINC-A free database of commercially available compounds for virtual screening. *J Chem Inf Model.* **2005**, *45*, 177-182.

(55) Ntie-Kang, F.; Zofou, D.; Babiaka, S.B.; Meudom, R.; Scharfe, M.; Lifongo, L.L.; Mbah, J.A.; Mbaze, L.M.; Sippl, W.; Efange, S.M. AfroDb: a select highly potent and diverse natural product library from African medicinal plants. *PLoS One* **2013**, *8*, e78085.

(56) Analyticon Discovery NP. Available online: http://www.ac-discovery.com/

(57) Kang, H.; Tang, K.; Liu, Q.; Sun, Y.; Huang, Q.; Zhu, R.; Gao, J.; Zhang, D.; Huang, C.; Cao, Z. HIM-herbal ingredients in-vivo metabolism database. *J Cheminform.* **2013**, *5*, 28.

(58) IBScreen NP. Available online: http://www.ibscreen.com

(59) Indofine Natural Products. Available online: http://www.indofinechemical.com

(60) NPACT Database. Available online: crdd.osdd.net/raghava/npact/

(61) Nubbe Natural Products. Available online: http://nubbe.iq.unesp.br

(62) Princeton NP. Available online: http://www.princetonbio.com

(63) Specs Natural Products. Available online: http://www.specs.net

(64) TCM Database@Taiwan. Available online: http://tcm.cmu.edu.tw

(65) UEFS Natural Products. Available online: http://www.uefs.br

(66) LigPrep, version 2.9, Schrödinger, LLC, New York, NY, **2014**.

(67) QikProp, Schrödinger, LLC, New York, NY, **2014**.

(68) Lipinski, C.A.; Lombardo, F.; Dominy, B.W.; Feeney, P.J. Experimental and computational approaches to estimate solubility and permeability in drug discovery and development settings. *Adv Drug Del Rev.* **1997**, *46*, 3-26.

(69) Berman, H.M.; Westbrook, J.; Feng, Z.; Gilliland, G.; Bhat, T.N.; Weissig, H.; Shindyalov, I.N.; Bourne, P.E. The Protein Data Bank. *Nucleic Acids Research* **2000**, *28*, 235-242.

(70) Schrödinger Suite 2016-3 Protein Preparation Wizard; Epik, Schrödinger, LLC, New York, NY, **2016**; Impact, Schrödinger, LLC, New York, NY, 2016; Prime, Schrödinger, LLC, New York, NY, **2016**.

(71) a) Friesner, R.A.; Banks, J.L.; Murphy, R.B.; Halgren, T.A.; Klicic, J.J.; Mainz, D.T.; Repasky, M.P.; Knoll, E.H.; Shelley, M.; Perry, J.K.; Shaw, D.E.; Francis, P.; Shenkin, P.S. Glide: a new approach for rapid, accurate docking and scoring. 1. Method and assessment of docking accuracy. *J Med Chem.* **2004**, *47*, 1739-1749; b) Glide, version 6.2, Schrödinger, LLC: New York, NY, USA, **2014**.

(72) a) Dixon, S.L.; Smondyrev, A.M.; Rao, S.N. PHASE: A Novel Approach to Pharmacophore Modeling and 3D Database Searching. *Chem Biol Drug Des.* **2006**, *67*, 370-372. b) Schrödinger Release 2016-4: Phase, Schrödinger, LLC, New York, NY, **2016**.

(73) Watts, K.S.; Dalal, P.; Murphy, R.B.; Sherman, W.; Friesner, R.A.; Shelley, J.C. ConfGen: a conformational search method for efficient generation of bioactive conformers. *J Chem Inf Model.* **2010**, *50*, 534-546.

(74) Hu, G.; Kuang, G.; Xiao, W.; Li, W.; Liu, G.; Tang, Y. Performance evaluation of 2D fingerprint and 3D shape similarity methods in virtual screening. *J Chem Inf Model.* **2012**, *52*, 1103-1113.

(75) Bowers, K.J.; Chow, E.; Xu, H.; Dror, R.O.; Eastwood, M.P.; Gregersen, B.A.; Klepeis, J.L.; Kolossvary, I.; Moraes, M.A.; Sacerdoti, F.D.; Salmon, J.K.; Shan, Y.; Shaw, D.E. Scalable algorithms for molecular dynamics simulations on commodity cluster. Proc. ACM/IEEE Conference on Supercomputing (SC06), **2006**, Tampa, FL.

(76) Corona, A.; Meleddu, R.; Esposito, F.; Distinto, S.; Bianco, G.; Masaoka, T.; Maccioni, E.; Menéndez-Arias, L.; Alcaro, S.; Le Grice, S. F.; Tramontano, E. Ribonuclease H/DNA Polymerase HIV-1 Reverse Transcriptase Dual Inhibitor: Mechanistic Studies on the Allosteric Mode of Action of Isatin-Based Compound RMNC6. *PLoS One* **2016**, *11,* e0147225.

(77) Palomba, M.; Rossi, L.; Sancineto, L.; Tramontano, E.; Corona, A.; Bagnoli, L.; Santi, C.; Pannecouque, C.; Tabarrini, O.; Marini, F. A new vinyl selenone-based domino approach to spirocyclopropyl oxindoles endowed with anti-HIV RT activity. *Org Biomol Chem.* **2016**, *14*, 2015-2024.

Supplementary Material - For Publication Online

Click here to download Supplementary Material - For Publication Online: Supplementary Material.docx